Süleyman Demirel Üniversitesi
Fen Bilimleri Enstitüsü Dergisi
Cilt 22, Sayı 2, 577-582, 2018

Süleyman Demirel University
Journal of Natural and Applied Sciences
Volume 22, Issue 2, 577-582, 2018

DOI: 10.19113/sdufbed.32580

Effect of Mg and Al Dual Doping on High Voltage Cycling of $LiNi_{0.4}Mn_{0.4}Co_{0.2}O_2$ Lithium-ion Battery Cathode Material

Muharrem KUNDURACI[*1]

[1]University of Turkish Aeronautical Association, Faculty of Engineering, Department of Mechanical Engineering, 06790, Ankara

(Alınış / Received: 12.02.2018, Kabul / Accepted: 04.06.2018, Online Yayınlanma / Published Online: 21.06.2018)

Keywords
Lithium-ion batteries,
Cathode,
High voltage,
Doping

Abstract: Nano-sized $LiNi_{0.4}Mn_{0.4}Co_{0.2}O_2$ lithium-ion battery cathode materials with and without dual Mg & Al doping were synthesized by Pechini method. The powdered materials were characterized using X-ray diffraction, scanning electron microscopy and electrochemical techniques. X-ray analyses showed that 003/104 peaks intensity ratio increased from 0.95 for undoped material to 1.27 for doped material, thereby suggesting that dual doping was beneficial in terms reducing Li/Ni cation mixing. Although dual doping caused some reduction in initial discharge capacity (140 vs. 128 mAh/g) and increase in charge transfer resistance relative to the undoped material, it noticeably helped increase capacity retention during battery testing at high voltage.

Mg ve Al Çifte Takviyenin $LiNi_{0.4}Mn_{0.4}Co_{0.2}O_2$ Lityum-iyon Pil Katot Malzemesinin Yüksek Voltaj Çevrimine Etkisi

Anahtar Kelimeler
Lityum-iyon piller,
Katot,
Yüksek voltaj,
Takviye

Özet: Nano boyutlu $LiNi_{0.4}Mn_{0.4}Co_{0.2}O_2$ lityum-iyon pil katot malzemeleri takviyesiz ve çifte Mg & Al takviyeli olarak Pechini yöntemi kullanılarak üretildi. Toz malzemeler X-ışını kırınımı, elektron mikroskobu ve elektrokimyasal tekniklerle incelendi. X-ışını analizleri 003/104 piklerin oranının takviyesiz malzemede 0.95'den takviyeli malzemede 1.27'ye çıktığını göstermiştir. Böylelikle çifte takviyenin Lityum/Nikel iyonların karışmasını azaltmada faydalı olduğu anlaşılmıştır. Çifte takviye takviyesiz malzemeye kıyasla ilk çevrim deşarj kapasitesinde azalmaya (140 vs. 128 mAh/g) ve empedansta artışa neden olmuş olsa da, yüksek voltajdaki pil testinde kapasite korunumunun artmasına yardımcı olduğu gözlenmiştir.

1. Introduction

Since their commercialization in 1991, the use of lithium-ion batteries expanded from consumer electronics to electric vehicles and stationary storage. Such advancement were fueled by the investigation of numerous research articles focusing on novel electroactive anode and cathode materials. These materials offered improved energy densities to satisfy the demands of emerging applications. On the cathode front, nickel-based layered type $LiNi_xMn_yCo_zO_2$ and $LiNi_xCo_yAl_zO_2$ materials stand out thanks to their high discharge capacities (>170 mAh/g) [1-6]. However, thermal safety and cycle life problems pose as the biggest problems to the use of high nickel (i.e. x>0.7). content cathode materials in electric vehicles. An alternative approach is based on the use of layered materials with low nickel content (i.e. x<0.5) but extending the upper cutoff voltage beyond 4.3 V. But, layered type cathode materials experience rapid capacity fade above 4.3 V due to structural instabilities associated with large volume changes and phase transformations as well as impedance increase due to the thickening of SEI layer [7]. Coating of cathode materials with a thin alumina layer by atomic layer deposition technique has been demonstrated to be conducive to cycling at high voltages [8-9]. However, such solutions can be expensive and not suited for mass production. An alternative approach is based on the use of small amounts of electrolyte additives with the intention to reduce unwanted side reactions on electrode surface due to the degradation of electrolyte at high voltages [10-11]. These remedies are aimed at controlling the surface chemistry of cathode material during cycling and do not deal with the structural degradations

* Corresponding author: kunduraci.m@hotmail.com

stemming from the extraction of excessive lithium at higher voltages. In this publication, dual doping of low nickel content $LiNi_{0.4}Mn_{0.4}Co_{0.2}O_2$ with magnesium and aluminum is reported for the first time. Magnesium doping is known to reduce the intermixing of lithium and nickel ions, thereby helping layered structure [12]. As for aluminum, it has been widely accepted to improve the structural stability of layered structure during lithium extraction [13]. The dual doped material will be shown to exhibit improved capacity retention at 4.45 V relative to the undoped cathode material.

2. Material ve Method

Doped and undoped $LiNi_{0.4}Mn_{0.4}Co_{0.2}O_2$ powders were produced using Pechini method. The process is summarized in Figure 1. Specifically, metal nitrate salts with desired stoichiometries were dissolved in minimum amount of dionized water. In a separate solution, citric acid was dissolved in ethylene glycol (1:4 mole ratio) at 110 °C on hot plate under stirring. The mole ratio of metal ions to citric acid was chosen to be 1. The aqueous solution was added dropwise to this solution until full completion. Later, the solution was heated further to 160 °C for esterification. Once the solution was fully dried, the powder was ground and heated to 800 °C in air for 20 hrs to obtain crystalline structures.

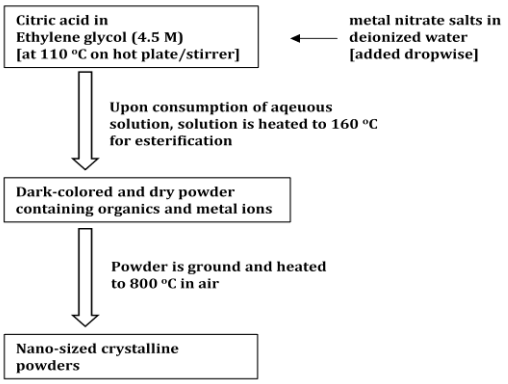

Figure 1. Schematic of Pechini process

The morphological properties of the cathode materials were studied using scanning electron microscope (SEM, FEI – Quanta 200 FEG) operated at 10 kV. Energy-dispersive X-ray spectroscopy (EDX) analysis was also performed for the elemental analyses. Powder X-ray diffraction was carried out by Panalytical X'pert Multi-Purpose and the patterns were collected in the range of 2θ = 15–70° using Bragg–Brentano geometry (Cu Kα radiation, **λ**= 0.15418 nm). The lattice constants *a* and *c* of cathode materials were calculated using equation 1 and diffraction angles of (003) and (104) peaks.

$$\frac{1}{d^2} = \frac{4}{3}\left(\frac{h^2 + hk + k^2}{a^2}\right) + \frac{l^2}{c^2} \qquad (1)$$

In equation 1, *h*, *k* and *l* represent the Miller indices and *d* is the spacing between (*hkl*) planes.

The lattice volumes of undoped and doped cathode materials were calculated using equation 2 since they belong to hexagonal crystal family.

$$V = \frac{a^2 \cdot c \cdot \sqrt{3}}{2} \qquad (2)$$

In order to prepare the cathode slurries, cathode material (70 wt%), conductive carbon Super P (10 wt%), PVDF binder (20 wt%) and NMP solvent were milled using steel balls for 15 min. NMP/PVDF weight ratio was chosen to be 20. The slurry was cast onto copper foil (12 μm in thickness) by doctor blade method. The casted electrode was vacuum dried overnight at 70 °C and then rapidly transferred into Argon filled glovebox (O_2 <0.5 ppm, H_2O <0.5 ppm) to prevent air exposure. Custom made cells were used to build lithium half cells in a two-electrode configuration. The separator was made of glass microfiber filter. The electrolyte was 1 M $LiPF_6$ in EC:DEC (1:1) solution. The cells were sealed after the assembly and rested at room temperature for 8 hours prior to testing. Electrochemical cycle life tests were conducted with Biologic MPG-2 battery tester. The cells were tested between 2.7 V and 4.3 V potential window in the first 20 cycles and between 2.7 V and 4.45 V in the following 20 cycles. The current density was kept constant at 75 mA/g (~C/2). The cathode active mass ranged from 5.9 to 6.1 mg/cm^2 in cells. AC impedance spectroscopy analyses were performed using the same unit by applying 5 mV alternating voltage. Cyclic voltammetry analysis was done at a scan rate of 0.2 mV/s between 2.7 V and 4.3 V.

3. Results

The X-ray diffraction spectra of undoped and Mg & Al dual doped $LiNi_{0.4}Mn_{0.4}Co_{0.2}O_2$ are presented in Figure 2. Both spectra were assigned to hexagonal R-3m space group. There is no sign of any secondary phase in both materials. The most noticeable difference between both spectra lies in the intensity ratios of (003) and (104) peaks. This ratio is often used as a gauge to judge the degree of intermixing (η) of nickel and lithium atoms at 3a and 3b lattices sites, respectively. For example η =5 means that 5% of lithium ions at 3b site is occupied by nickel ions. The intermixing is undesired since nickel ions on lithium site block the migration of Li+ during cell charging and discharging, thereby hurting battery performance. The dramatic improvement in 003/104 peak ratio (Table 1) proves the stucture enhancing benefits of magnesium and aluminum doping. Based on available literature data on NCM type layered materials, η was estimated to be 5-6% for undoped cathode and 2-3% for doped cathode materials [14-15].

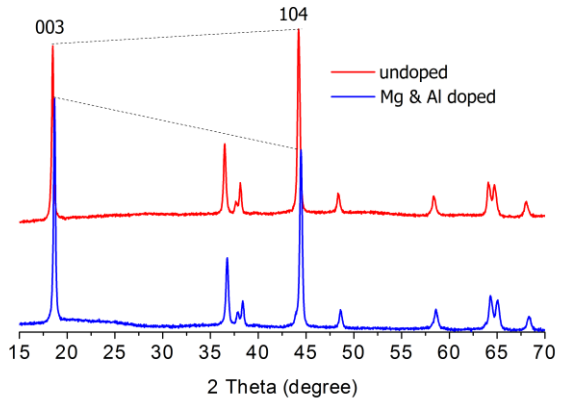

Figure 2. X-ray diffraction spectra of undoped and doped $LiNi_{0.4}Mn_{0.4}Co_{0.2}O_2$ cathode materials

The calculated lattice constants and cell volume values are provided in Table 1. The decrease in cell volume upon doping can be attributed to two factors; introduction of smaller ionic radius Al^{3+} (50 ppm) into layered structure and decrease in intermixing [14].

Table 1. Summary of X-ray diffraction results for undoped Mg & Al dual doped $LiNi_{0.4}Mn_{0.4}Co_{0.2}O_2$

symbol	undoped	doped	unit
a	2.8779	2.8675	Å
c	14.385	14.245	Å
unit cell volume	103.2	101.4	$Å^3$
003/104 peak ratio	0.95	1.27	-
η	5-6	2-3	%

Morphological characteristics of cathode materials were studied using scanning electron microscope. The images of undoped and doped powder materials are provided in Figure 3. Both materials consist of nanosized primary particles with diameters in the range of 100-300 nm, suggesting that particle size will not be a distingushing factor in battery testing results. Also, the materials seem to be non-aggregated. These structures can be expected to show no significant lithium-ion transport limitation at 0.5C charge/discharge rates.

Energy dispersive elemental analyses were also performed to ascertain the exact chemical composition of cathode materials. Based on these results, the composition of undoped and doped cathode materials are found to be $LiNi_{0.39}Mn_{0.41}Co_{0.2}O_2$ and $LiNi_{0.384}Mn_{0.361}Co_{0.21}Mg_{0.013}Al_{0.041}O_2$, assuming 1:1 mole ratio of lithium to total metal atoms.

In order to get a more accurate description of chemical compostions, ICP-OES (inductively coupled plasma optical emission spectroscopy) was utilized. The exact compositions were found to be $LiNi_{0.42}Mn_{0.38}Co_{0.2}O_2$ and $LiNi_{0.40}Mn_{0.37}Co_{0.20}Mg_{0.01}Al_{0.02}O_2$ for undoped and doped materials, respectively. They are in good agreement with EDS results.

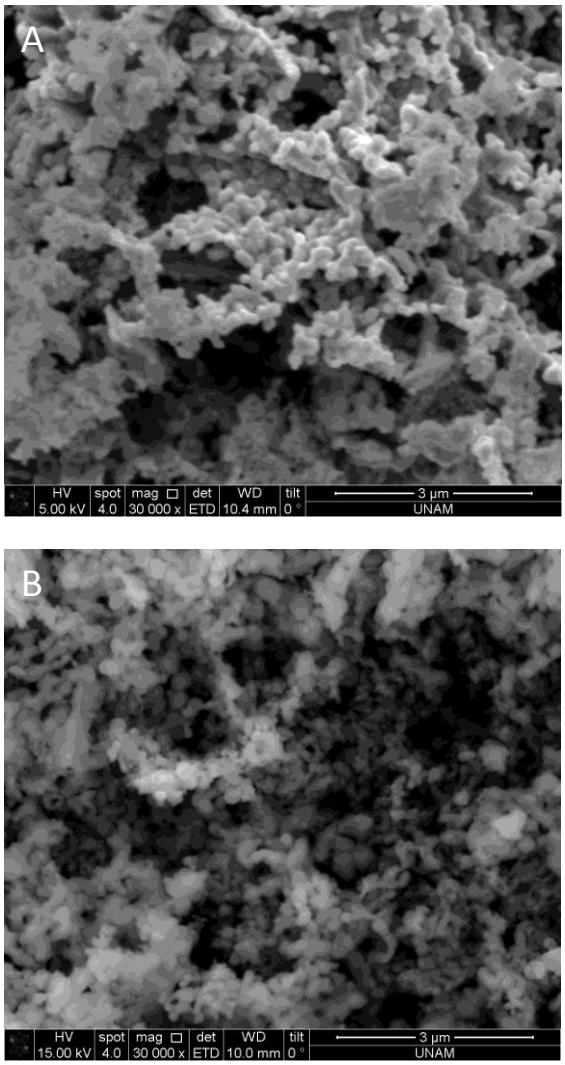

Figure 3. Scanning electron microscopy images of a) undoped and b) Mg & Al doped $LiNi_{0.4}Mn_{0.4}Co_{0.2}O_2$ cathode materials

The battery cells made of undoped or doped $LiNi_{0.40}Mn_{0.4}Co_{0.2}O_2$ cathode materials were galvanostatically charged and discharged between 2.7 V and 4.3 V at ~0.5C rate for 20 cycles. Their first cycle charge and discharge voltage profiles are in Figure 4. The discharge capacity of undoped material is 140 mAh/g while it is 128 mAh/g for Mg & Al doped cathode material. The first cycle discharge capacity of undoped material is in line with previous literature. A comparison of literature data is provided in Table 2.

Table 2. List of some literature studies reporting discharge capacity values of $LiNi_{0.4}Mn_{0.4}Co_{0.2}O_2$ Li-ion battery cathode materials

Discharge capacity (mAh/g)	Voltage range	Current rate	Reference
155-160	2.5 – 4.3 V	C/2	15
142-156	2.5 – 4.4 V	C/10	16
145	2.5 - 4.6 V	C/2	17
180	2.5 – 4.5 V	C/2	18
145-150	3.0 – 4.3 V	C/2	19
140	3.0 – 4.3 V	C/2	This work

The biggest reason of decrease in capacity upon doping can be explained by the electrochemically inactive nature of dopants, amounting to 3-5 mole percentage of total metal ions. The introduction of these dopants will reduce the concentration of electrochemically active nickel and cobalt ions, thereby hurting capacity. The other reason could be the lower electronic conductivity of doped material. The doped material is of brown color while undoped material is black (direct current electronic conductivity measurements performed on powders revealed that undoped material's conductivity is 1.5 times that of doped material). On the other hand, the first cycle coulombic efficiencies (83.1% for undoped and 82.7% for doped) and the shape of voltage profiles are almost identical. This suggests that the dopants do not interfere with the mechanism of (de)lithiation processes.

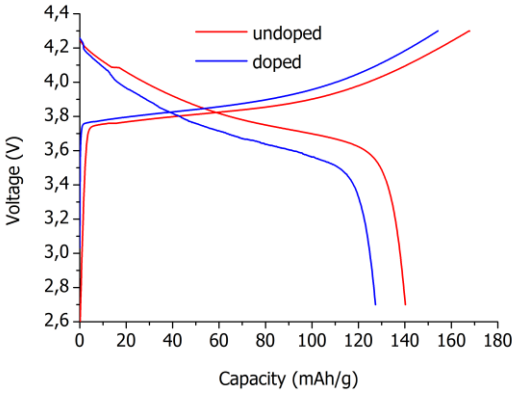

Figure 4. First cycle charge and discharge voltage profiles of undoped and Mg & Al doped $LiNi_{0.4}Mn_{0.4}Co_{0.2}O_2$ cathode materials

Cyclic voltammetry analysis was performed in order to have a better comparison of charge and discharge mechanisms in undoped and doped cathode materials. Their profiles are provided in Figure 5. Each cathode material has one main oxidation and reduction peaks, implying that the mechanisms of (de)lithiation are the same for both cathode materials. However, the peaks shift to higher voltages in Mg & Al dual doped cathode material due to inductive effect [20]. The increase in charge potential in doped material can be partially responsible for smaller capacity of this material as lesser amount of lithium ions will be extracted from doped material when the cutoff charge potential is reached. The other noticeable difference between undoped and doped cathode materials is the distance between oxidation and reduction peaks. The potential difference is 0.29 V for doped material and 0.26 V for undoped material. The larger difference for doped material suggests slower kinetics for this material.

The evolution of discharge capacities and percentage capacity retention numbers for cathode materials are shown in Figure 6 and 7, respectively. In the first 20 cycles, both materials experience similar capacity

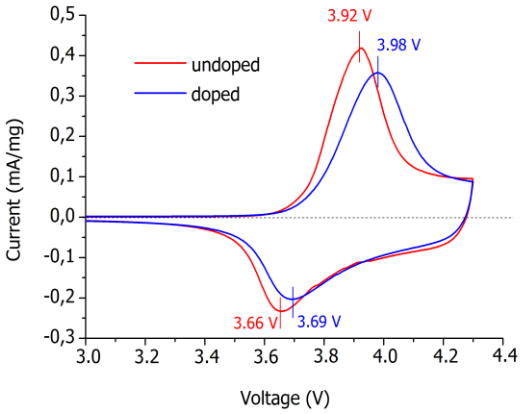

Figure 5. Cyclic voltammetry profiles of undoped and Mg & Al doped $LiNi_{0.4}Mn_{0.4}Co_{0.2}O_2$ cathode materials

fading rates. Specifically, the average fading rate is 0.52% per cycle for doped material and 0.6% for undoped material. Upon increasing the charge (delithiation) cutoff voltage to 4.45 V, the discharge capacities of both cathode materials rise initially due to the extraction of more lithium ions from layered structure. The increase is 11 and 14 mAh/g for undoped and doped cathode materials, respectively. However, in the following 20 cycles the capacity loss accelerates for undoped $LiNi_{0.40}Mn_{0.40}Co_{0.2}O_2$ material to 0.94% but stays relatively same at 0.58% for Mg & Al doped cathode material. Battery cycling results demonstrate without doubt that Mg & Al dual doping helps with capacity retention numbers of layered cathode material.

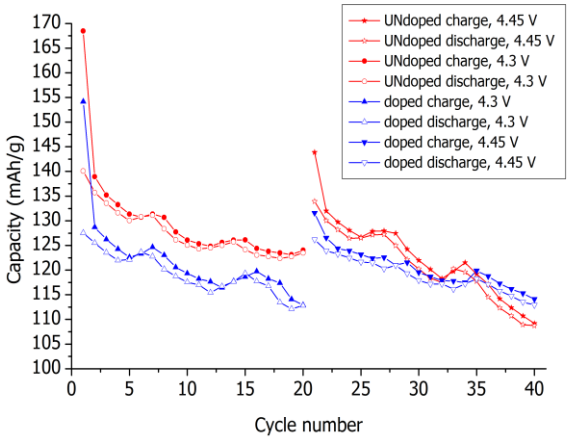

Figure 6. Charge and Discharge capacity values of undoped and Mg & Al doped $LiNi_{0.4}Mn_{0.4}Co_{0.2}O_2$ cathode materials at 75 mA/g current density. Voltage range was 2.7-4.3 V for cycle numbers 1-20 and 2.7-4.45 V for cycle numbers 21-40

In order to explain the origin of such improvement, impedance spectroscopy analyses of cells were performed before the start of cycling and after 40 cycles. The Z-plot data of cells are given Figure 8. An equivalent circuit model was added to explain each component. The resistance at high frequencies (R1) corresponds to the diffusion resistance of lithium ions in electrolyte and is equal for each cell as

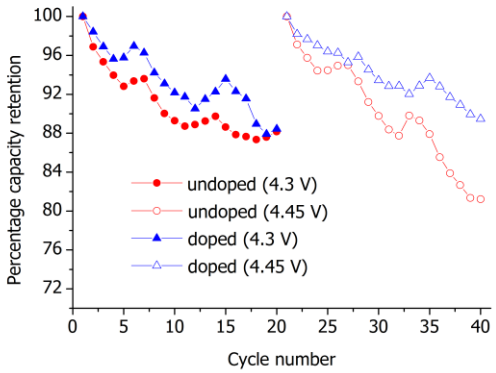

Figure 7. Percent capacity retention values of cells for undoped (sphere) and Mg & Al doped (triangle) $LiNi_{0.4}Mn_{0.4}Co_{0.2}O_2$ cathode materials. The values were normalized with respect to the capacities at 1st and 21st cycles. Voltage range was 2.7-4.3 V for cycle numbers 1-20 and 2.7-4.45 V for cycle numbers 21-40

expected. R2 and CPE are charge transfer resistance and non-ideal double-layer capacitance, respectively. Finally, Warburg impedance is the impedance of Li+ diffusion in bulk material. At the fresh states, undoped and doped $LiNi_{0.4}Mn_{0.4}Co_{0.2}O_2$ have charge transfer values of 110 and 160 ohms, respectively. The larger number for Mg & Al doped cathode most likely stems from its lower electronic conductivity and consistent with cyclic voltammetry results. After 40 cycles, however, the resistance values increase by 44% for doped cathode and 80% undoped cathode materials. This result is in agreement with galvanostatic cell measurements.

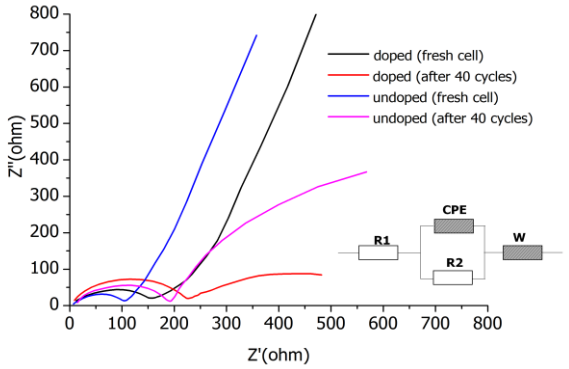

Figure 8. Z-plots of half cells made of undoped and doped cathode materials before cycling and after 40 cycles. The inset represents the equivalent circuit model

4. Discussion and Conclusion

Nanosized layered type $LiNi_{0.42}Mn_{0.38}Co_{0.2}O_2$ and $LiNi_{0.40}Mn_{0.37}Co_{0.20}Mg_{0.01}Al_{0.02}O_2$ lithium-ion battery cathode materials were synthesized by a wet-chemistry method. Battery half cells made of these materials were evaluated at 4.3 V and 4.45 V cutoff voltages and compared for their lithium capacities and capacity retention values. Although dual-doped material had smaller first cycle discharge capacity than baseline cathode material (128 vs. 140 mAh/g), it exhibited improved high voltage percentage capacity retention. Specifically, the capacity fading rate of doped material was 0.58% as opposed 0.94% for undoped control material when cycled between 3.0 V and 4.45 V regime. In literature encompassing battery cathode materials, several factors have been proposed to explain the origin of improved cycling stabilities including smaller volume change, smaller impedance growth thanks to better passivation of cathode surface layer and more stable lattice structure upon [21-23]. Our impedance tests showed that the rate of impedance build-up on cathode surface was smaller in case of doped material. More extensive studies such as in-situ X-ray diffraction or ex-situ TEM will be needed to ascertain the major cause of better high voltage cycling stability upon Mg and Al doping.

Acknowledgment

The author likes to thank Prof. Dr. Kadri Aydinol from METU for allowing him to use his laboratory for the synthesis and electrochemical evaluation of cathode materials. X-ray diffraction and SEM-EDX analyses were performed at UNAM-Bilkent University. ICP-OES measurements were carried out at METU central laboratory. The project did not receive any government or private funding.

References

[1] Pan L., Xia Y., Qiu B., Zhao H., Guo H., Jia K., Gu Q., Liu Z. 2016. Synthesis and electrochemical performance of micro-sized Li-rich layered cathode material for Lithium-ion batteries. Electrochimica Acta, 211(2016), 507-514.

[2] Kang J., Pham H., Kang D., Park H., Song S. 2016. Improved rate capability of highly loaded carbon fiber-interwoven $LiNi_{0.6}Co_{0.2}Mn_{0.2}O_2$ cathode material for high-power Li-on batteries. Journal of Alloys and Compounds, 657(2016), 464-471

[3] Yoo G., Jang B., Son J. 2015. Novel design of core shell structure by NCA modification on NCM cathode material to enhance capacity and cycle life for lithium secondary battery. Ceramics International, 41(2015), 1913-1916

[4] Hwang I., Lee C., Kim J., Yoon S. 2012. Particle size effect of Ni-rich cathode materials on lithium ion battery performance. Materials Research Bulletin, 47(2012), 73-78

[5] Cho Y., Lee Y., Park S., Lee Y., Cho J. 2010. $LiNi_{0.8}Co_{0.15}Al_{0.05}O_2$ cathode materials prepared by TiO_2 nanoparticle coatings on $Ni_{0.8}Co_{0.15}Al_{0.05}(OH)_2$ precursors. Electrochimica Acta, 56(2010), 333-339

[6] Liu S., Xiong L., He C. 2014. Long cycle life lithium ion battery with lithium nickel cobalt manganese oxide (NCM) cathode. Journal of Power Sources, 261(2014), 285-291

[7] Zhu Y., Luo X., Zhi H., Yang X., Xing L., Liao Y., Xu M., Li W. 2017. Structural exfoliation of layered cathode under high voltage and its suppression by interface film derived from electrolyte additive. ACS Applied Materials and Interfaces, 9(2017), 12021-12034

[8] Zhou A., Liu Q., Wang W., Yao X., Hu W., Zhang L., Yu X., Li J., Li H. 2017. Al_2O_3 surface coating on $LiCoO_2$ through a facile and scalable wet-chemical method towards high-energy cathode materials withstanding high cutoff voltages. Journal Materials Chemistry A, 5(2017), 24361-24370

[9] Wise A., Ban C., Weker J., Misra S., Cavanagh A., Wu Z., Li Z., Whittingham M., Xu K., George S., Toney M. 2015. Effect of Al_2O_3 coating on stabilizing $LiNi_{0.4}Mn_{0.4}Co_{0.2}O_2$ cathodes. Chemistry of Materials, 27(2015), 6146-6154

[10] Madec L., Ma L., Nelson KJ., Petibon R., Sun JP., Hill IG., Dahn JR. 2016. The effects of a ternary electrolyte additive system on the electrode/electrolyte interfaces in high voltage lithium-ion cells. Journal of The Electrochemical Society, 163(2016), A1001-A1009

[11] Ma L., Xia J., Dahn JR. 2014. Improving the high voltage cycling of $LiNi_{0.42}Mn_{0.42}Co_{0.16}O_2$ (NMC442)/Graphite pouch cells using electrolyte additives. Journal of The Electrochemical Society, 161(2014), A2250-A2254

[12] Huang Z., Wang Z., Zheng X., Guo H., Li X., Jing Q., Yang Z. 2015. Structural and electrcohemical properties of Mg-doped nickel based cathode materials $LiNi_{0.6}Co_{0.2}Mn_{0.2-x}Mg_xO_2$ for lithium ion batteries. RSC Advances, 5(2015), 88773-88779

[13] Couceiro A., Garcia S., Rodriquez M., Soulette F., Julien C. 2002. Effect of the aluminum doping on the microstructure and morphology of $LiNi_{0.5}Co_{0.5}O_2$ oxides. Ionics, 8(2002), 192-200

[14] Julien C., Mauger A., Zaghib K., Groult H. 2016. Optimization of layered cathode materials for lithium-ion batteries. Materials, 9(2016), 595.

[15] Ngala J., Chernova N., Ma M., Mamak M., Zavalij P., Whittingham M. 2003. The synthesis, characterization and electrochemical behavior of the layered $LiNi_{0.4}Mn_{0.4}Co_{0.2}O_2$ compound. Journal of Materials Chemistry, 14(2003), 214-220.

[16] Channu VSR., Ravichandran D., Rambabu B., Holze R. 2014. Nanocrystalline $LiNi_{0.4}Mn_{0.4}Co_{0.2}O_2$ cathode for lithium-ion batteries. Colloids and Surfaces A, 453(2014), 125-131

[17] Ma M., Chernova NA., Toby BH., Zavalij PY., Whittingham M. 2007. Structural and electrochemical behavior of $LiNi_{0.4}Mn_{0.4}Co_{0.2}O_2$. Journal of Power Sources, 165(2007), 517-534

[18] Shi SJ., Mai YJ., Tang YY., Gu CD., Wang XL., Tu JP. 2012. Preparation and electrochemical performance of ball-like $LiNi_{0.4}Mn_{0.4}Co_{0.2}O_2$ cathode materials. Electrochimica Acta, 77(2012), 39-46

[19] Myung ST., Lee KS., Sun YK., Yashiro H. 2011. Development of high power lithium-ion batteries: layer $Li[Ni_{0.4}Mn_{0.4}Co_{0.2}]O_2$ and spinel $Li[Li_{0.1}Al_{0.05}Mn_{1.85}]O_4$. Journal Power Sources, 196(2011), 7039-7043

[20] Kuznetsov DA., Han B., Yu Y., Rao RR., Hwang J., Leshkov YR., Horn YS. 2018. Tuning redox reactions via inductive effect in metal oxides and complexes, and implications in oxygen electrocatalysis. Joule, 2(2018), 225-244

[21] Ishidzu K., Oka Y., Nakamura T. 2016. Lattice volume change during charge/discharge reaction and cycle performance of $Li[Ni_xCo_yMn_z]O_2$. Solid State Ionics, 288(2016), 176-179

[22] Li P., Xue L., Li Y., Su Q., Chen Y., Cao G., Lei T., Zhu J., Deng S. 2017. Modification of $LiNi_{0.5}Co_{0.2}Mn_{0.3}O_2$ cathode material using nano TiO_2 to enhance the cycle stability in high-voltage ranges. Materials Letters, 207(2017), 217-220

[23] Uzun D. 2015. Boron-doped $Li_{1.2}Mn_{0.6}Ni_{0.2}O_2$ as a cathode active material for lithium ion battery. 2015. Solid State Ionics, 281(2015), 73-81